Biochemistry

 Volume 41, Number 31 August 6, 2002

Articles

Mechanism of *Thermoanaerobacterium saccharolyticum* β-Xylosidase: Kinetic Studies†

David J. Vocadlo, Jacqueline Wicki, Karen Rupitz, and Stephen G. Withers*

Protein Engineering Network of Centres of Excellence of Canada and Department of Chemistry, University of British Columbia, Vancouver, British Columbia, Canada V6T 1Z1

Received January 24, 2002; Revised Manuscript Received May 8, 2002

ABSTRACT: The catalytic mechanism of *Thermoanaerobacterium saccharolyticum* β-xylosidase (XynB) from family 39 of glycoside hydrolases has been subjected to a detailed kinetic investigation using a range of substrates. The enzyme exhibits a bell-shaped pH dependence of k_{cat}/K_m, reflecting apparent pK_a values of 4.1 and 6.8. The k_{cat} and k_{cat}/K_m values for a series of aryl xylosides have been measured and used to construct two Brønsted plots. The plot of log(k_{cat}/K_m) against the pK_a of the leaving group reveals a significant correlation ($\beta_{lg} = -0.97$, $r^2 = 0.94$, $n = 8$), indicating that fission of the glycosidic bond is significantly advanced in the transition state leading to the formation of the xylosyl−enzyme intermediate. The large negative value of the slope indicates that there is relatively little proton donation to the glycosidic oxygen in the transition state. A biphasic, concave-downward plot of log(k_{cat}) against pK_a provides good evidence for a two-step double-displacement mechanism involving a glycosyl−enzyme intermediate. For activated leaving groups (pK_a < 9), the breakdown of the xylosyl−enzyme intermediate is the rate-determining step, as indicated by the absence of any effect of the pK_a of the leaving group on log(k_{cat}) ($\beta_{lg} \approx 0$). However, a strong dependence of the first-order rate constant on the pK_a value of relatively poor leaving groups (pK_a > 9) suggests that the xylosylation step is rate-determining for these substrates. Support for the dexylosylation chemical step being rate-determining for activated substrates comes from nucleophilic competition experiments in which addition of dithiothreitol results in an increase in turnover rates. Normal secondary α-deuterium kinetic isotope effects ($^{\alpha-D}$(V) or $^{\alpha-D}$(V/K) = 1.08−1.10) for three different substrates of widely varying pK_a value (5.15−9.95) have been measured and these reveal that the transition states leading to the formation and breakdown of the intermediate are similar and both steps involve rehybridization of C1 from sp^3 to sp^2. These results are consistent only with "exploded" transition states, in which the saccharide moiety bears considerable positive charge, and the intermediate is a covalent acylal-ester where C1 is sp^3 hybridized.

The major component of plant cell wall hemicelluloses is the polymer xylan. This molecule is composed of a backbone of β-1,4-linked D-xylopyranosyl units decorated with a variety of sugars including L-arabinose and D-glucuronic acid. The enzymatic degradation of xylans has attracted the attention of the pulp and paper industry because it has been

† Financial assistance from the Protein Engineering Network of Centres of Excellence of Canada (PENCE) and the Natural Sciences and Engineering Research Council of Canada (NSERC) is gratefully acknowledged. D.J.V. was supported by scholarships from NSERC and the Science Council of British Columbia.

* To whom correspondence should be addressed. Fax (604) 822-8869. E-mail: withers@chem.ubc.ca.

10.1021/bi020077v CCC: $22.00
Published on Web 07/09/2002

shown that the "biobleaching" of paper-pulp is effective in terms of decreasing both cost and environmental impact (*1*). The complete digestion of xylan requires the action of many enzymes, including xylanases, which hydrolyze the xylan backbone to yield shorter, soluble oligosaccharides, and β-xylosidases, which liberate xylose from the nonreducing termini of these soluble xylo-oligosaccharides.

β-Xylosidases are currently classified into families 3, 39, 43, 52, and 54 of glycoside hydrolases (*2*). These enzymes may operate by one of two mechanisms, one of which results in inversion of configuration at the anomeric center while the other results in retention of stereochemistry at that center. Mechanistic studies of β-xylosidases have been limited to family 43 xylosidases, which are known to utilize an inverting mechanism (*3*, *4*) and, recently, a retaining xylosidase of unknown classification (*5*).

Family 39 of glycoside hydrolases, of which *Thermoanaerobacterium saccharolyticum* β-xylosidase (XynB) is a member, contains both bacterial β-D-xylosidases and mammalian α-L-iduronidases (*6*). Members of this family, by extension from stereochemical studies with *T. saccharolyticum* β-xylosidase, utilize a retaining catalytic mechanism (Scheme 1) (*7*). In the vast majority of cases where the catalytic mechanism of a retaining glycosidase has been investigated, two carboxyl groups have been found to be the catalytic residues (*8*). One functions as a nucleophile, attacking the anomeric center to displace the leaving group and form a covalent glycosyl−enzyme intermediate. In XynB, this residue has been identified as E277 using the mechanism-based inactivator 2,4-dinitrophenyl 2-deoxy-2-fluoro-β-D-xyloside (*9*). The other critical residue acts as a catalytic acid/base that provides, in the first step, protonic assistance to facilitate departure of the leaving group. In the second step, this residue acts as a base catalyst that assists in the hydrolysis of the xylosyl−enzyme intermediate by promoting the attack of water on the anomeric center. On the basis of studies with the family 39 β-xylosidase from *Bacillus stearothermophilus*, Bravman et al. have very recently proposed the highly conserved E160 as the catalytic acid/base residue of *T. saccharolyticum* β-xylosidase (*10*).

A mechanism involving an ion-pair intermediate is still invoked in the literature for β-retaining glycosidases (*11*−*13*) despite the increasing body of information pointing to a covalent glycosyl−enzyme intermediate (*14*, *15*). This paper describes the first detailed mechanistic study of a cloned retaining β-xylosidase, providing strong evidence indicating that the catalytic mechanism of this enzyme proceeds by a covalent xylosyl−enzyme intermediate.

EXPERIMENTAL PROCEDURES

Reagents, Enzymes, and Bacterial Strains. Growth media components were obtained from Difco. Plasmid-containing strains were grown in Luria Broth containing 50 μg/mL kanamycin (LB_{kan}) or in TYP (16 g/L tryptone, 16 g/L yeast extract, 5 g/L NaCl, 2.5 g/L K_2HPO_4) containing 50 μg/mL kanamycin (TYP_{kan}). *Pwo* DNA polymerase and deoxynucleoside triphosphates were obtained from Boehringer Mannheim. Restriction endonucleases and T4 DNA ligase were from New England BioLabs. *Escherichia coli* Topp10 cells and the pZeroBlunt cloning kit were from Invitrogen. The pET-29b(+) expression vector, *E. coli* BL21(DE3) cells, and His-Bind metal chelation resin were obtained from Novagen. The *E. coli* JM110 cells (*rpsl*, (Str^r), *thr*, *leu*, *thi-1*, *lacY*, *galK*, *galT*, *ara*, *tonA*, *tsx*, *dam*, *dcm*, *supE44*, Δ(*lac-proAB*), and [F′ *traD36 proAB lac*^{q}ZΔ*M15*]) were from Stratagene. PCR DNA fragment purification and plasmid purification kits were from Qiagen and Promega. Preparation of oligonucleotide primers and DNA sequencing was performed at the Nucleic Acids and Peptide Service facility (NAPS), University of British Columbia.

Amplification and Subcloning of xynB. The gene encoding the His_6-tagged β-xylosidase gene from *T. saccharolyticum* (*xynB*) was amplified via polymerase chain reaction (PCR). The PCR mixture contained 10 μM oligonucleotide primers (shown below), 1 mM concentrations of the four deoxynucleoside triphosphates in 100 μL of DNA polymerase buffer and 50 ng of plasmid pXPH3, a generous gift from

Scheme 1: Proposed Catalytic Mechanism for *T. saccharolyticum* β-Xylosidase (XynB) Showing a Covalent α-Xylosyl−Enzyme Intermediate[a]

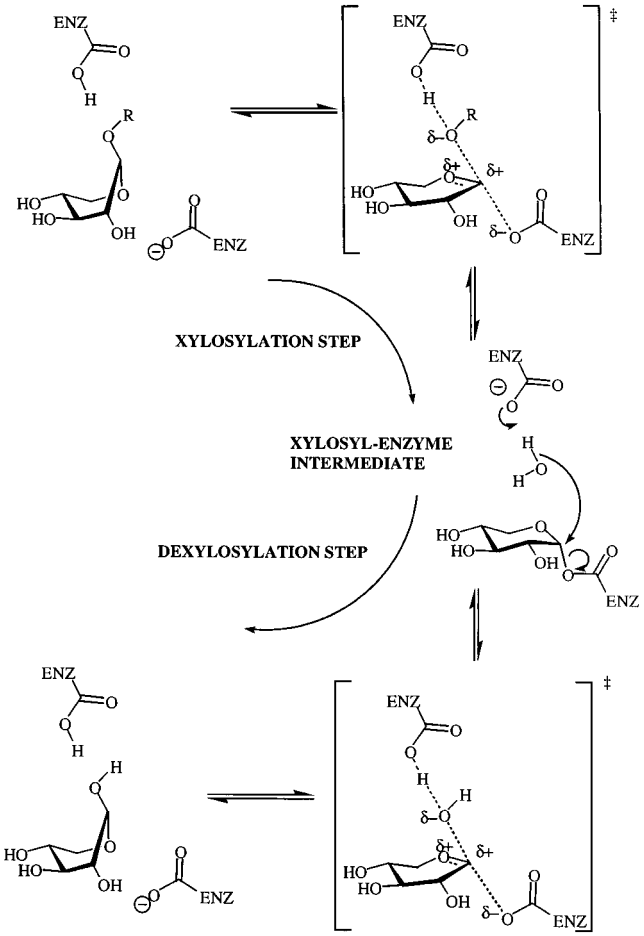

[a] For XynB, the xylosylation step is rate-determining for substrates bearing relatively basic aryl leaving groups ($pK_a > 9$), and the dexylosylation step is rate-determining for substrates bearing activated, less basic, leaving groups ($pK_a < 9$).

[1] Abbreviations: 2FDNPX, 2,4-dinitrophenyl 2-deoxy-2-fluoro-β-D-xylopyranoside; 2,5DNPX, 2,5-dinitrophenyl β-D-xylopyranoside; 3,4DNPX, 3,4-dinitrophenyl β-D-xylopyranoside; *p*NPX, *para*-nitrophenyl β-D-xylopyranoside; *o*NPX, *ortho*-nitrophenyl β-D-xylopyranoside; *m*NPX, *meta*-nitrophenyl β-D-xylopyranoside; PX, phenyl β-D-xylopyranoside; *o*NHAcX, *ortho*-acetamidophenyl β-D-xylopyranoside; *p*OMeX, *para*-methoxyphenyl β-D-xylopyranoside; 3,5DiClX, 3,5-dichlorophenyl β-D-xylopyranoside; 3,4DiMeX, 3,4-dimethylphenyl β-D-xylopyranoside; XynB, *Thermoanaerobacterium saccharolyticum* β-xylosidase.

Dr. J. Gregory Zeikus (Department of Biochemistry, Michigan State University, East Lansing, MI). Plasmid pXPH3 contains a 2-kb *Pst*I−*Hind*III fragment of *T. saccharolyticum* DNA, carrying a 1500 bp open reading frame that contains the entire *xynB* gene. After heating the reaction mixture to 95 °C, the PCR reaction was started by adding 5 units of *Pwo* DNA polymerase (Boehringer Mannheim). Thirty PCR cycles (45 s at 94 °C, 45 s at 56 °C, and 70 s at 72 °C) were performed in a thermal cycler (Perkin-Elmer, GeneAmp PCR System2400). Agarose gel electrophoresis of the PCR product revealed a single DNA fragment of approximately 1500 bp as estimated by gel electrophoresis.

The forward primer was as follows:

5′-TAA CAT ATG ATT AAA GTA AGA GTG CCA GAT TTT-3′
*Nde*I

The reverse primer was as follows:

5′-TAA CTC GAG ATA TCC ATT TAT CTT GCT ATC-3′
*Xho*I

After purification of the PCR product using the Qiaquick PCR purification kit according to the manufacturer's protocol (Qiagen), a blunt-end ligation into plasmid pZero2.0 was performed according to the manufacturer's protocol (Invitrogen). Electrocompetent Topp10 cells (Invitrogen) were subsequently transformed with the ligation mixture using a BioRad GenePulser II. Single colonies were selected and grown overnight in $LB_{Zeocin+kan}$, and DNA was isolated via minipreparation technique (Promega Wizard *Plus* kit). Restriction endonuclease mapping revealed positive clones, which were subsequently sequenced to verify the published sequence of *xynB*.

The cloned *xynB* in pZero2.0 was cut out using the unique sites engineered into the oligonucleotide primers (see above). The His_6-fusion protein expression vector, pET-29b(+) (Novagen), was also digested with *NdeI* and *XhoI*. A ligation reaction was performed at a ratio of 10:1 (insert to vector) using gel-purified DNA fragments and T4 DNA ligase (1 unit/10 ng of DNA) at 25 °C. The cloned product, called pET29x*ynB*H_6, was subsequently transformed into electrocompetent Topp10 cells, selected by the kanamycin resistance conferred by pET-29b(+). Single colonies were selected and grown overnight in LB_{kan}, and DNA was isolated via the minipreparation technique. Restriction endonuclease mapping revealed positive clones. Topp10 transformed cells were used for preparation of large amounts of plasmid pET29*xynBH*$_6$ (Qiagen Plasmid Maxi kit) and long-term storage of the vector as glycerol stock.

Overexpression and Purification of His_6-Tagged XynB. The constructed pET29*xynBH*$_6$ expression vector was used to transform electrocompetent BL21(DE3) cells. The *E. coli* transformants were selected on LB_{kan} (50 μg/mL) agar plates. A single colony was picked and grown overnight in 3 mL of LB_{kan}, and this culture was subsequently used to inoculate 1 L of TYP_{kan}. After the culture grew to an OD_{600} of 2−3 at 30 °C, 0.4 mM isopropyl β-D-thiogalactoside (IPTG) was added to induce protein expression from the *lac* promoter and grown for an additional 4 h at 25 °C. Overexpression of the enzyme was monitored by sampling of both induced and noninduced cells using SDS-polyacrylamide gel electrophoresis. Induced cells were then harvested and suspended in 30 mL of binding buffer (5 mM imidazole, 500 mM NaCl, 20 mM Tris-HCl, pH 7.9). The cell suspension was passed two times through a French press at 0−5 °C and centrifuged at 10 000*g* for 30 min at 4 °C to yield soluble cell extract. A 20 mL slurry of His-Bind resin (nitriloacetic acid-agarose, Novagen) was placed into a 50 mL column, yielding a bed volume of 10 mL. The column was washed with 10 bed volumes of sterile, deionized water and then charged with nickel by adding 5 bed volumes of 50 mM $NiSO_4$. Unbound Ni^{2+} was washed away with 5 bed volumes of binding buffer (see above). The soluble cell extract from a 1 L cell culture was applied to the column. The column was washed with 5 bed volumes of binding buffer. $XynBH_6$ protein was eluted from the Ni^{2+} column with a linear imidazole gradient from 30 to 200 mM in a buffer containing 500 mM NaCl and 20 mM Tris-HCl (pH 7.9). Fractions (3 mL) were collected (1.0 mL/min flow rate) and assayed for xylosidase activity using *p*NPX. Active fractions were further analyzed using SDS−polyacrylamide gel electrophoresis. Fractions containing pure enzyme were pooled and stored at 4 °C. The extinction coefficient (ϵ_{280}) determined for $XynBH_6$ by active site titration using 2,4-dinitrophenyl 2-deoxy-2-fluoro-β-D-xyloside (2FDNPX) is 3.19 mL mg^{-1} cm^{-1}. The enzyme was concentrated to ∼2.4 mg/mL using a Centriprep concentrator (30 kDa cutoff) from Amicon and dialyzed using a Slide-A-Lyzer (10 kDa cutoff) from Pierce against 50 mM sodium phosphate buffer pH 7.00.

General Procedures and Synthesis. All buffer chemicals and other reagents were obtained from the Sigma/Aldrich Chemical Co. unless otherwise noted. Details pertaining to the synthesis of the compounds used in this study and characterization of the compounds can be found in the Supporting Information.

Enzyme Kinetics. The concentration of $XynBH_6$ active sites was determined by titrating samples of the enzyme with 2FDNPX at a concentration (0.57 mM) in large excess of enzyme (0.0025−0.01 mM). Solutions containing the inactivator in 50 mM sodium citrate buffer, pH 5.5, were equilibrated in a 1 cm path length quartz cell at 37 °C in the cell-holder for 10 min prior to addition of the enzyme. After addition of the enzyme, the absorbance of the solution at 400 nm was monitored over time until it was evident that it had reached a slow steady state. Corrections were made for the initial absorbance of the xyloside sample.

Michaelis−Menten parameters for aryl glycosides were determined by continuous measurement of the release of the substituted phenol product using a Pye-Unicam PU8700 spectrophotometer as described previously (*16*, *17*). Reactions were monitored at appropriate wavelengths using the extinction coefficients given in the Supporting Information. Phenol pK_a values used were those reported in Kempton and Withers (*16*). Unless indicated otherwise, the reaction mixtures, in 50 mM sodium citrate buffer, pH 5.5, containing 0.1% BSA (buffer A) at 37 °C, were preincubated in the cell-holder for 10 min prior to addition of enzyme. For nucleophilic competition experiments, DTT was included in mixtures as indicated and care was taken to ensure the desired pH of the assay mixture was obtained and that the rate of spontaneous hydrolysis was less than 5% of the enzymatic rate. The concentrations of 2,5DNPX and PX used in the nucleophilic competition experiments were 237 μM and 5.15 mM, respectively. Enzyme-catalyzed hydrolysis for each

substrate was measured at 8−10 different substrate concentrations ranging from about 0.14K_m to 7K_m, where practical. Values for K_m and k_{cat} were determined from the initial rates of hydrolysis (V_0) versus substrate concentration by nonlinear regression analysis using the computer program GraFit 4.0 (*18*). In cases where significant transglycosylation was observed, a nonlinear regression was performed on data from 0.14K_m to approximately 2K_m. The values of k_{cat} and K_m so obtained were then compared to those determined from linear regression of the reciprocal data as plotted according to Lineweaver−Burke.

Isotope effects were determined in two different ways due to limitations arising from the K_m values of each substrate investigated. For *o*NPX (K_m = 46 μM) and 2,5DNPX (K_m = 11 μM), saturation conditions were readily obtained, and therefore, $^{\alpha-D}$(V) isotope effects were determined. Accurate determinations of the $^{\alpha-D}$(V/K) isotope effects for 2,5DNPX and *o*NPX was precluded by the low concentration of substrate required (0.1K_m to 0.2K_m) for these experiments and the consequent poor signal-to-noise in the progress curves. Conversely, for *p*NHAcX, the relatively high K_m (8.1 mM) prohibited measurement of the $^{\alpha-D}$(V) isotope effect due to the limited solubility of the substrate. Thus, for this substrate, the $^{\alpha-D}$(V/K) isotope effect was determined by continuously monitoring the depletion of a low concentration of substrate (1/18 × K_m) in the reaction at 287 nm. Quartz cells (1 cm path length) were filled with a solution containing buffer A (pH 5.5) equilibrated at 37 °C and either the enzyme (0.0037 mg/mL with 2,5DNPX; 0.0084 mg/mL with *p*NPX; 0.125 mg/mL with *o*NHAcX) or substrate (4.1 mM *o*NPX; 0.25 mM 2,5DNPX; 0.46 mM *o*NHAcX). The reaction was initiated by the addition either of an aliquot (20 μL) of thermally equilibrated substrate (*o*NPX or 2,5DNPX) or of enzyme (in the case of *o*NHAcX). Initial rates (for *o*NPX and 2,5DNPX) or second-order rate constants (for *o*NHAcX) were measured alternately for protio and deuterio samples until at least eight rates of each had been determined. Average rates or rate constants were then calculated for the protio and deutero substrates and the ratio was taken to yield the isotope effect. ^{1}H NMR analysis of the deuterated substrates revealed that the extent of isotopic incorporation was greater than 95%.

pH Dependence of k_{cat}/K_m. The k_{cat}/K_m values for the hydrolysis of *p*NPX at each pH value were determined from progress curves at low substrate concentrations as follows. A solution containing *p*NPX (8 μM, 0.2 × K_m), 0.1% BSA, and the appropriate buffer was warmed to 37 °C. The reaction was initiated by the addition of a 10 μL aliquot that contained sufficient amounts of the enzyme (0.2−2.36 mg/mL) to ensure that 5−7 half-lives had passed within 5−10 min of starting the reaction. The reaction was monitored continuously at 360 nm, and after the reaction was judged to be complete, the pH of the mixture was checked, and it was established that no significant change in pH had occurred during the course of the assay. The change in absorbance with time was fitted to a first-order rate equation using the program GraFit 4.0 (*18*), yielding values for the pseudo-first-order rate constant at each pH value. Since at low substrate concentrations ([S] ≪ K_m), the reaction rates are given by the equation

$$v = k_{cat}[E][S]/K_m \quad (1)$$

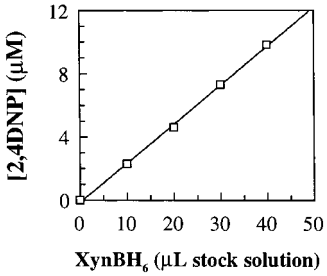

FIGURE 1: Active site titration of *T. saccharolyticum* β-xylosidase using 2FDNPX as an active site titrant.

the k_{obs} values correspond to $[E]_o k_{cat}/K_m$. Thus, k_{cat}/K_m values can be extracted by division of these obtained rate constants by the enzyme concentration. The buffers used each contained 0.1% BSA (w/v) and were as follows: pH 4.5−6.5, 50 mM citrate and 150 mM sodium chloride; pH 6.5−8.0, 50 mM phosphate and 150 mM sodium chloride; pH 8.0−9.5, 50 mM AMPSO and 150 mM sodium chloride. By analyzing the bell-shaped k_{cat}/K_m versus pH plots using GraFit 3.0, we assigned two apparent pK_a values of ionizable groups. Enzyme stability over the pH range and assay time of the study was examined by adding enzyme at the same concentration as was used in the pH study to a preincubated cell containing 0.1% BSA and the appropriate buffer at 37 °C. After 10 min, 1 aliquot of the mixture was removed and injected into another preincubated solution of *p*NPX (600 μM), 50 mM sodium citrate buffer pH 5.5. In all cases, no more than 11% enzyme death had occurred over a period of 10 min.

RESULTS

Active Site Titration. 2,4-Dinitrophenyl 2-deoxy-2-fluoro-β-D-glycosides have been shown to be effective mechanism based inactivators of β-retaining glycosidases (*8*). For each equivalent of XynB that reacted with 2FDNPX, one equivalent of DNP is released. The resulting fluoroglycosyl−enzyme intermediate turns over only very slowly (*9*). Incubation of $XynBH_6$ with 2FDNPX results in its stoichiometric labeling as confirmed by ESI-MS (data not shown) indicating that 100% of the enzyme is properly folded and functional. The number of enzyme active sites and its extinction coefficient can thus be determined by monitoring the DNP released spectrophotometrically at several different enzyme concentrations. A plot of the volume of enzyme solution added against the final change in absorbance at 400 nm arising from stoichiometric release of the DNP moiety is shown in Figure 1 and allows the calculation of an experimental extinction coefficient of 3.19 mL mg^{-1} cm^{-1}. This value was used in all experiments to evaluate the amount of enzyme used. The stock of enzyme was periodically assayed to determine whether the second-order rate constant for a fixed amount of enzyme remained constant. In this way it was established that $XynBH_6$ was stable for at least 6 months when stored in the elution buffer of the metal chelate affinity column.

Substrate Specificity. Kinetic parameters for a series of substrates are presented in Table 1. From examination of the rate constant governing the hydrolysis of a series of aryl glycosides, it can be seen that the enzyme has considerable specificity for xylosides over all other substrates tested, which is consistent with earlier qualitative observations (*19*).

Table 1: Michaelis-Menten Parameters for the Hydrolysis of a Series of *p*-Nitrophenyl Glycosides by *T. saccharolyticum* β-Xylosidase

phenyl glycoside substrate	k_{cat} (s^{-1})[a]	K_m (mM)[a]	k_{cat}/K_m (s^{-1} mM^{-1})
β-*p*NPX	9.7	0.036	270
α-*p*NPX	undetectable	N/A	N/A
α-*p*NPAra	~1.0	~3.0	~0.33
β-*p*NPGlc	0.18	7.4	0.024
β-*p*NPFuc	0.082	~17	~0.006
β-*p*NPGal	undetectable	N/A	N/A
β-*p*NPGlcNAc	undetectable	N/A	N/A

[a] Errors in kinetic parameters are less than 10% except in cases where approximate values are indicated.

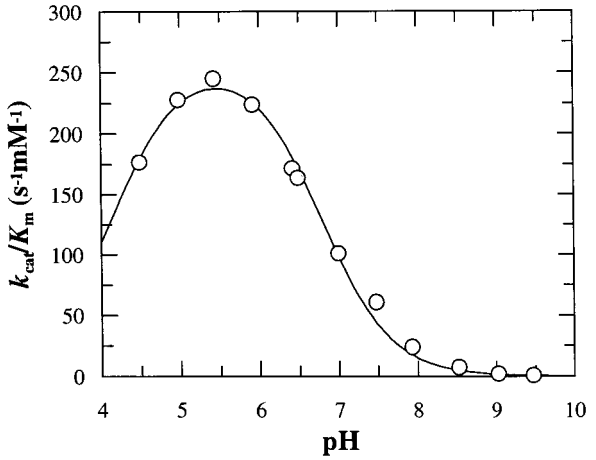

FIGURE 2: pH dependence for the hydrolysis of *p*NPX catalyzed by *T. saccharolyticum* β-xylosidase.

pH Dependence. Values of k_{cat}/K_m at a series of pH values between 4.5 and 9.5 were determined. K_m was also determined at the extreme pH values to ensure that its value was maintained significantly above the substrate concentration used in the study. These values are plotted in Figure 2. Values of k_{cat}/K_m depend on two ionizations, and the apparent pK_a values of these titratable groups could be extracted as pK_{a1} = 4.1 and pK_{a2} = 6.8. The value of pK_{a1} is somewhat unreliable, as the data for this limb of the pH profile could not be completed owing to instability of the enzyme at lower pH.

Substrate Reactivity. The consequences on the Michaelis−Menten parameters of change in the phenolate structure are shown in Table 2, where k_{cat} and K_m for series of aryl xylosides with a range of differing phenol leaving group abilities (as measured by pK_a of the phenol) are presented. At higher concentrations, substrates bearing activated leaving groups with pK_a values of less than 9.0 show significant deviation from Michaelian saturation kinetics. However, substrates with pK_a values higher than 9 show normal saturation kinetics. Examples of the Michaelis−Menten plots of substrates bearing a leaving group with either a low or a high pK_a value are shown in Figure 3. Values of k_{cat} and K_m for all substrates showing non-Michaelian kinetics were determined by nonlinear fitting of data to substrate concentrations lower than those levels where significant deviation from Michaelian kinetics is observed (Figure 3). Such data fitting was in good accord with the values obtained by linear regression of the low concentration linear portion of the Lineweaver−Burk plots. These results are plotted in the form

Table 2: Michaelis−Menten Parameters for the Hydrolysis of a Series of Aryl Xylosides by *T. saccharolyticum* β-Xylosidase

substrate	pK_a	k_{cat} (s^{-1})[a]	K_m (mM)[a]	k_{cat}/K_m (s^{-1} mM^{-1})
2,5DNPX	5.15	7.3	0.011	670
3,4DNPX	5.36	8.9	0.0099	900
*p*NPX	7.18	9.7	0.036	270
*o*NPX	7.22	9.9	0.046	220
3,5DClPX	8.19	7.7	0.035	220
*m*NPX	8.39	11	0.15	73
3ClPX	9.02	10	0.29	36
4BrPX	9.34	1.7	0.34	5.1
NapX	9.51	2.6	0.31	8.5
*o*NHAcX[b]	9.96	~14	~8	1.8
PX	9.99	4.0	1.9	2.1
*p*OMePX	10.20	1.1	0.22	5.2
3,4DMePX	10.32	1.6	2.5	0.65

[a] Errors in kinetic parameters are less than 10%. [b] The limited solubility of this substrate allowed only for an estimation of k_{cat} and K_m.

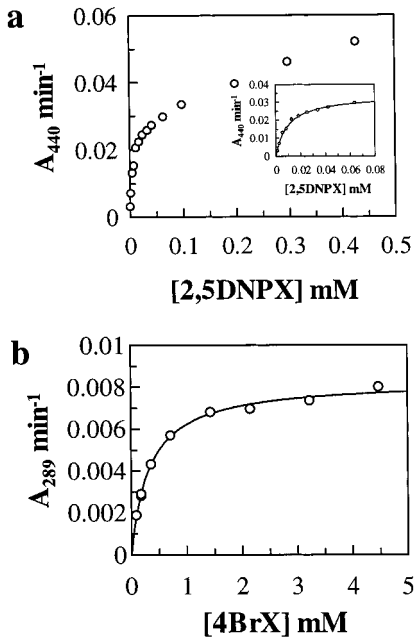

FIGURE 3: Michaelis−Menten plots and detail of the low substrate concentration range (inset) for the *T. saccharolyticum* β-xylosidase catalyzed hydrolysis of (a) a substrate for which dexylosylation is rate-determining, 2,5DNPX, and (b) a substrate for which xylosylation is rate-determining, 4BrPX.

of Brønsted relationships in Figure 4. Secondary kinetic isotope effects on three different substrates with aryl leaving groups of widely varying pK_a values (5.15−9.95) have also been determined, and these are shown in Table 3, along with the pK_a values of the substrate leaving groups.

Nucleophilic Competition. The values of k_{cat} for 2,5DNPX and PX were determined at varying concentrations of the competitive nucleophile DTT and are shown in Figure 5. A clear increase in k_{cat} with increasing nucleophile concentration is seen for 2,5DNPX, but no increase is observed for PX. Michaelis−Menten parameters were determined at three different concentrations of DTT in order to determine the effect of DTT upon K_m. These data are listed in Table 4.

DISCUSSION

Detailed understanding of the kinetic and chemical mechanisms of an enzyme require dissection of the pH-

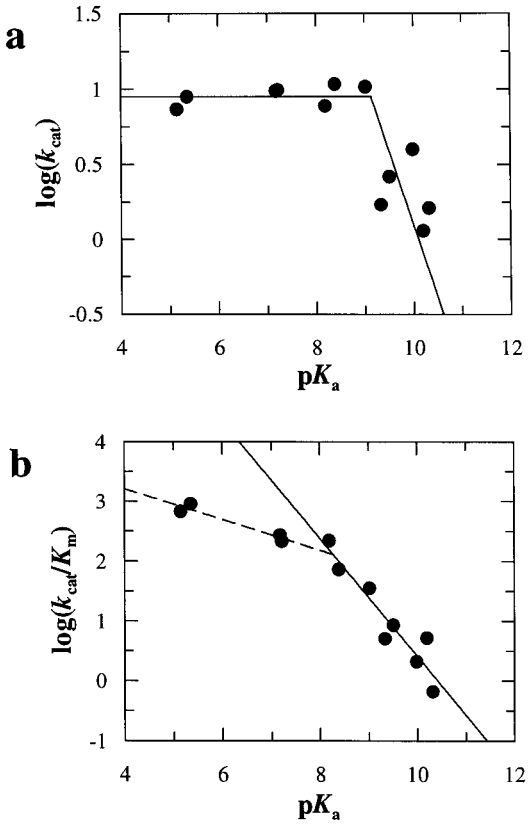

FIGURE 4: Brønsted plots relating the rate of *T. saccharolyticum* β-xylosidase catalyzed hydrolysis of a series of aryl xylosides with the pK_a of the corresponding phenol. (a) Plot of log(k_{cat}) vs pK_a of the aglycone leaving group. (b) Plot of log(k_{cat}/K_m) vs pK_a of the aglycon phenol.

Table 3: Secondary Deuterium Kinetic Isotope Effects Measured with *T. saccharolyticum* β-Xylosidase

substrate	pK_a	RDS[a]	k_H/k_D
2,5DNPX	5.15	dexylosylation	1.10 ± 0.01 (V)
*o*NPX	7.22	dexylosylation	1.09 ± 0.02 (V)
*o*NHAcX	9.95	xylosylation	1.08 ± 0.03 (V/K)

[a] RDS: Rate-determining step.

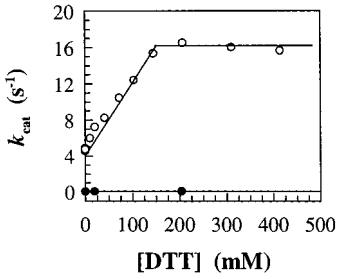

FIGURE 5: Values of k_{cat} for the *T. saccharolyticum* β-xylosidase-catalyzed hydrolysis of (○) 2,5DNPX and (●) PX at different DTT concentrations.

dependence, identification of the rate-determining steps for a series of substrates, and probing of the transition states for these steps. Such an analysis follows.

pH Profile. The pH dependence of the second-order rate constant k_{cat}/K_m for the hydrolysis of *p*NPX reveals ionizations occurring within the free enzyme. A bell-shaped pH profile similar to that obtained in this study has been observed for several β-retaining glycosidases (*16*, *20*, *21*). The large half-height width ($\Delta pK_a = 2.7$) of the bell-shaped profile

Table 4: Kinetic Parameters for the *T. saccharolyticum* β-Xylosidase-Catalyzed Hydrolysis of 2,5DNPX at Different DTT Concentrations

[DTT] (mM)	k_{cat} (s^{-1})	K_m (μM)	k_{cat}/K_m (s^{-1} mM^{-1})
0	4.0 ± 0.2	22 ± 3	180 ± 30
20	8.2 ± 0.5	49 ± 9	170 ± 30
62	13.1 ± 0.4	57 ± 6	230 ± 30
169	26.9 ± 0.9	146 ± 16	180 ± 20

suggests that these apparent pK_a values likely reflect intrinsic pK_a values of the ionizable residues, although the possibility of reverse protonation (see the following companion paper for a detailed discussion of reverse protonation) makes firm assignments impossible (*22*, *23*). NMR titration studies of the ionizable groups in another β-retaining glycosidase (*Bacillus circulans* xylanase) reveal that the two apparent pK_a values associated with the inflections in bell-shaped profiles of k_{cat}/K_m versus pH reflect the ionizations of the two key active site carboxyl groups (*24*, *25*). One of the carboxyl groups in this study has a significantly perturbed apparent pK_a value (6.8) compared to that of a normal carboxylic acid residue (4.8), as has been seen in many glycosidases (*16*, *17*, *26*). The other residue has an estimated apparent pK_a (4.1) consistent with that expected for a carboxylic acid (4.8). By analogy with previous studies, it would seem likely that these apparent pK_a values reflect the intrinsic pK_a values of the nucleophile (4.1) and acid/base (6.8) residues. Such an assignment, however, cannot be made conclusively in the absence of further studies owing to the above-mentioned possibility of reverse protonation. Such studies are described in a companion paper immediately following. Regardless of this ambiguity, for the purpose of determining the pH at which the enzyme has optimal activity, this study provides the necessary information to proceed with more detailed mechanistic work.

Substrate Specificity. From examination of the rate constants governing the hydrolysis of a series of *para*-nitrophenyl glycoside substrates, it can be seen that the enzyme has considerable specificity for xylosides over all other substrates tested (Table 1), which is consistent with earlier qualitative observations (*19*). Xylosidases from families 43 (*27*) and 54 (*5*) have been shown to have a relaxed specificity for α-L-arabinosides (the C4 epimer of β-D-xylosides). These enzymes often cleave the arabinosides at rates similar to, or even greater (*27*) than, those for β-xylosides. The lower relative activity of $XynBH_6$ toward α-L-arabinosides suggests that $XynBH_6$ recognizes O4 more stringently than do xylosidases from other families. Specificity is even greater at other positions, as the enzyme does not readily accommodate any increased steric bulk at C5 and C2 as evidenced by the much lower rate constants for the hydrolysis of fuco-, gluco-, and 2-acetamido-glucosides.

Proposed Mechanism of Action. The most widely accepted mechanism of action of β-retaining glycosidases that cleave the glycosidic linkage with retention of configuration is similar to that postulated by Koshland in 1953 (*28*). This involves the initial binding of the substrate to the enzyme in a distorted conformation in which the leaving group is held in a pseudoaxial position with the pyranose ring adopting a sofa or $^{4,1}B$ conformation (*29*). Subsequently, the general acid/base catalytic residue donates a proton to the glycosidic

Scheme 2: Kinetic Mechanism of *T. saccharolyticum* β-Xylosidase

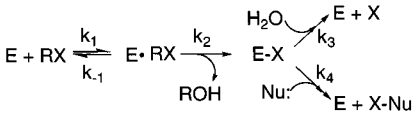

oxygen as C1 undergoes electrophilic migration to form a bond with the anionic catalytic nucleophile. The glycosyl−enzyme intermediate so formed has been found most commonly to adopt a $^4C_1$ conformation, although the −1 xylopyranose rings of the glycosyl−enzymes formed on two family 11 xylanases have both been shown to adopt a $^{2,5}B$ conformation (*30*, *31*). Interestingly, family 39 contains only β-xylosidases, which cleave substrates lacking the hydroxymethyl group found in D-hexopyranosides, and α-L-iduronidases, which also act on substrates with high conformational flexibility. In the case of the iduronidase, distortion of the sugar ring to a $^{2,5}B$ conformation would place the bulky carboxyl substituent in an equatorial position. An entertaining possibility is that such conformational flexibility and/or lack of a hydroxymethyl group may favor the evolution of a mechanism in which the intermediate adopts a $^{2,5}B$ conformation. At this stage, however, no information is available concerning the conformation adopted in enzymes of this family. Regardless, the covalent glycosyl−enzyme is then hydrolyzed by base-catalyzed attack of water at the anomeric center to form a β-sugar hemiacetal product and return the enzyme to its resting protonation state.

Evidence for a Two-Step Mechanism Involving Oxocarbenium Ion-Like Transition States. Structure/Reactivity Studies. A biphasic concave downward Brønsted plot (Figure 4) of log(k_{cat}) against pK_a of the leaving group suggests a two-step ping-pong mechanism as shown in Scheme 2. Similar biphasic Brønsted plots have been observed with the β-retaining glucosidases from *Agrobacterium* sp. (*16*) and sweet almonds (*32*). Conversely, for the retaining β-xylosidase from *Trichoderma koningii*, no dependence of rate on leaving group reactivity was observed (*5*).

The first step (k_2), the xylosylation step, involves cleavage of the glycosidic bond and formation of the xylosyl−enzyme intermediate. Substrates with good leaving groups (pK_a < 9) show no dependence of their reactivity on phenol leaving group ability. Therefore, for these activated substrates, the xylosylation step is unlikely to be rate-determining although it is possible that a nonchemical step, such as product dissociation, is rate-determining with these activated substrates. However, good evidence pointing to a rate-determining chemical step is found in the nucleophilic competition experiments when DTT is added as an exogenous nucleophile to the reaction mixture. A large, linear increase in the value of k_{cat} for the enzyme-catalyzed hydrolysis of 2,5DNPX is observed as the DTT concentration is increased. This suggests that DTT efficiently intercepts the xylosyl−enzyme intermediate and accelerates its breakdown by a competing alternate pathway governed by k_4 and DTT concentration (Scheme 2). At DTT concentrations greater than approximately 150 mM, there is no additional effect on k_{cat}, indicating that the rate of dexylosylation has been increased such that the rate of dexylosylation step is either greater than or equivalent to that of the xylosylation step. Confirmation of this interpretation arises from examining the Michaelis−Menten parameters for the hydrolysis of 2,5DNPX by $XynBH_6$ in the presence of 20, 62, and 169 mM DTT. K_m can be expressed as

$$K_m = \left(\frac{k_{-1} + k_2}{k_1}\right)\left(\frac{(k_3 + [\mathrm{DTT}]k_4)}{(k_3 + [\mathrm{DTT}]k_4) + k_2}\right) \qquad (2)$$

Thus, when k_3 is much less than k_2, K_m is small. As (k_3+[DTT]k_4) increases relative to k_2, K_m also increases to a point at which (k_3+[DTT]k_4) ≫ k_2, and K_m can then be simplified to the form

$$K_{m(max)} = \left(\frac{k_{-1} + k_2}{k_1}\right) \qquad (3)$$

K_m as expressed in eq 3 reflects the maximum value of the Michaelis constant ($K_{m(max)}$) with any substrate for which there is not a rapid equilibrium between the Michaelis complex and the free enzyme and substrate. Therefore, as the concentration of DTT is increased and the dexylosylation step proceeding by both pathways (Scheme 2; Path A (k_3) and Path B ([DTT]k_4)) accelerates, an increase in the value of K_m is observed. No effect on the first step is expected, and this is borne out by the absence of any significant change in k_{cat}/K_m, a parameter that presumably reflects the first irreversible step of the reaction. The lack of dependence of the rate of hydrolysis of PX (Figure 5) on DTT concentration lends further support for this interpretation (Figure 5). There is no significant change in the value of k_{cat} even at 202 mM DTT. Since the xylosylation step is rate-limiting for PX, this confirms that DTT acts only to accelerate the dexylosylation step of the reaction by intercepting the xylosyl−enzyme intermediate, with no effect on the xylosylation step. A value for k_4 (0.07 $s^{-1}mM^{-1}$) can be estimated from the region of Figure 5 that shows a linear dependence on DTT concentration. Another estimate for k_4 (0.06 $s^{-1}mM^{-1}$) can be obtained using eq 2 and making the following assumptions: $k_2 \approx k_{cat}$ as determined in the presence of DTT concentrations greater than 150 mM, $k_3 \approx k_{cat}$ determined in the absence of DTT, and $(k_{-1} + k_2)/k_1 \approx K_m$ in the presence of DTT concentrations greater than 150 mM. Together, these data clearly show that, under the conditions studied here, only the chemical steps are rate-determining and the biphasic nature of the plot is a consequence of a change in rate-determining step from xylosylation (for substrates bearing a leaving group with a pK_a value of >9) to dexylosylation (for substrates bearing a leaving group with a pK_a value of <9).

A hydroxyl group from another saccharide moiety can also act in the place of water to intercept the covalent xylosyl−enzyme intermediate (Scheme 2, Path B). This transglycosylating ability has been observed in many retaining glycosidases and the capacity for XynB to partition the intermediate in this way has been previously documented (*7*). On incubating the enzyme in the presence of substrates bearing leaving groups with either high (PhX) or low pK_a (2,5DNPX) values disaccharide products are observed by mass spectrometric and TLC analysis (data not shown). Substrates that bear phenolic leaving groups with pK_a values greater than 9, for which the rate-determining step is the formation of the intermediate, yield Michaelian kinetics (Figure 3a). Substrates bearing a phenolic leaving group of less than 9, for which the rate-determining step is deglyco-

sylation, exhibit non-Michaelian kinetics (Figure 3a). This can be attributed to an increase in the rate of breakdown of the xylosyl−enzyme intermediate via transglycosylation in the presence of elevated concentrations of aryl xylosides. This transglycosylation must occur for all substrates since there is a common intermediate, yet is only observed in the kinetic data for those substrates for which the rate-determining step is dexylosylation (leaving group $pK_a < 9$).

A biphasic plot is also observed if $\log(k_{cat}/K_m)$ is plotted against the pK_a value of the phenol leaving group. The region of the Brønsted plot for substrates bearing relatively poor leaving groups ($pK_a > 8$) reveals a significant correlation between the pK_a value of the leaving group phenol and $\log(k_{cat}/K_m)$ as can be seen from the slope ($r^2 = 0.94$, $n = 8$) of $\beta_{lg} = -0.97$ in Figure 4. The parameter k_{cat}/K_m governs the reaction of the free enzyme to the transition state of the first irreversible step along the reaction pathway, regardless of the pK_a of the leaving group, while k_{cat} only governs this step when substrates bearing poor leaving groups ($pK_a > 9$) are used. We can expect, therefore, that the negative β_{lg} value determined from the plot of $\log(k_{cat}/K_m)$ should correlate with the region of the plot of $\log(k_{cat})$ involving substrates having leaving group pK_a values of greater than 9.0, and indeed, this is the case. Such a large negative β_{lg} indicates that there is significant fission of the glycosidic bond in the transition state and that there is relatively little proton donation to the developing phenolate anion. The observation of almost complete breakage of the glycosidic linkage is consistent with the isotope effects, which indicate that the pyranose ring has significant oxocarbenium ion character at the transition state (vide infra).

Unexpectedly, however, the slope of the Brønsted plot of $\log(k_{cat}/K_m)$ becomes less negative for xylosides with good leaving groups. Such behavior has also been observed in the Brønsted plots of $\log(k_{cat}/K_m)$ constructed for the hydrolysis of aryl glycosides by other β-retaining glycosidases, including the glucosidases from *Agrobacterium* sp. (*16*) and sweet almonds (*32*) and a xylanase from *Cellulomonas fimi* (*17*). As k_{cat}/K_m reflects the first irreversible chemical step, one would expect a linear correlation through all pK_a values. The biphasic nature of this plot may therefore arise from the first step becoming reversible as the pK_a of the leaving group decreases. Early studies on the inhibition of sweet almond β-glucosidase showed that the K_i values of phenols were dependent on their pK_a values with lower pK_a phenols being more effective inhibitors (*33*). Thus, it is possible that with lower pK_a phenols the off rate for dissociation of the phenol from the enzyme is slowed and internal return occurs with the liberated phenol collapsing with the xylosyl−enzyme intermediate to regenerate the aryl xyloside substrate. This would make the first step reversible, and consequently, k_{cat}/K_m might not reflect solely the xylosylation step. An alternative explanation may be that *ortho*-substituted phenolic aglycones result in steric congestion within the active site, thereby preventing efficient positioning of enzymic groups and resulting in a decrease in the rate of the xylosylation step. The apparent absence of any such effects using *ortho*-nitrophenyl β-D-xylopyranoside, however, suggests that such effects are not pronounced.

Kinetic Isotope Effects. α-Deuterium-kinetic isotope effects have been used to probe changes in hybridization at the anomeric center for both enzyme-catalyzed and spontaneous hydrolysis of glycosides. Such measurements monitor the change in hybridization on going from a stable species (ground state, Michaelis complex, or glycosyl−enzyme intermediate) to the subsequent transition state. 1-^{2}H-substituted substrates were prepared that incorporate leaving groups with a large range of leaving group pK_a values in order to determine the change in hybridization for the xylosylation step (first transition state), the dexylosylation step (second transition state), and a near borderline case. In all three cases, a significant normal isotope effect of $k_H/k_D \approx 1.09$ is observed. From the Brønsted plots, we know that k_{cat} for both *p*NPX and 2,5DNPX must reflect the second chemical step (dexylosylation). As discussed above, k_{cat}/K_m reflects the first irreversible chemical step, and for *o*NHAcX (leaving group $pK_a = 9.95$) this is clearly the xylosylation step.

From the studies outlined above, we can be confident that chemical steps investigated for each of these substrates are entirely rate-determining and consequently the measured isotope effects should reflect the intrinsic isotope effects. The KIE values measured are in the range measured for other glycosidases on both the glycosylation (1.05−1.11) and deglycosylation steps (1.08−1.25) (*16*, *17*, *34*, *35*). The normal isotope effects observed for both steps of the reaction indicate a change in hybridization of C1 from sp^3 to sp^2 in both steps. Such changes in hybridization are consistent only with a covalent sp^3 hybridized xylosyl−enzyme intermediate and cannot be reconciled with an oxocarbenium ion intermediate. The isotope effects for the two steps are relatively large and of very similar magnitude, indicating that the transition states for both steps have significant oxocarbenium ion character. This result, in conjunction with a β_{lg} of −0.97, indicates that the transition states leading to the formation and breakdown of the covalent xylosyl−enzyme intermediate are "exploded" with very little nucleophilic participation.

CONCLUSIONS

All of the data reported here support a two-step double-displacement mechanism for the family 39 XynB enzyme in which a covalent xylosyl−enzyme is formed and hydrolyzed with acid/base catalytic assistance. The transition states bracketing the intermediate are "exploded" with considerable oxocarbenium ion-like character and very little nucleophilic participation. Such a mechanism is very similar to the A_ND_N mechanism found for the hydrolysis of glycosyl fluorides in the presence of anionic nucleophiles (*36*). The reaction therefore very likely proceeds by an enforced preassociation or a concerted mechanism involving electrophilic migration of C1 from bonded contact to bonded contact through a highly cationic transition state (*15*).

ACKNOWLEDGMENT

The authors would like to thank Dr. Tony Warren for providing laboratory space and equipment, Dr. J. Gregory Zeikus for the generous gift of plasmid pXPH3, Shouming He for technical assistance, and Dr. L. Ziser and Lloyd MacKenzie for providing some of the aryl xyloside substrates.

SUPPORTING INFORMATION AVAILABLE

Details pertaining to the synthesis and characterization of the compounds used in this study, as well as the extinction

coefficients and assay wavelengths used in the kinetic analyses are provided as Supporting Information. This material is available free of charge via the Internet at http://pubs.acs.org.

REFERENCES

1. Joseleau, J. P., Comtat, J., and Ruel, K. (1992) in *Xylans and Xylanases* (Visser, J., Beldman, G., Someren, M. A. K. v., and Voragen, A. G. J., Eds.) pp 1−15, Elsevier, Amsterdam.
2. Coutinho, P. M., and Henrissat, B. (1999) Carbohydrate-Active Enzymes, (http://afmb.cnrs-mrs.fr/~cazy/CAZY/index.html, accessed Jan 2002).
3. Kasumi, T., Tsumuraya, Y., Brewer, C. F., Kersters-Hilderson, H., Claeyssens, M., and Hehre, E. J. (1987) *Biochemistry 26*, 3010−3016.
4. Padmaperuma, B., and Sinnott, M. L. (1993) *Carbohydr. Res. 250*, 79−86.
5. Li, Y.-K., Yao, H.-J., and Pan, I.-H. (2000) *J. Biochem. (Tokyo) 127*, 315−320.
6. Henrissat, B., and Bairoch, A. (1993) *Biochem. J. 293*, 781−788.
7. Armand, S., Vielle, C., Gey, C., Heyraud, A., Zeikus, J. G., and Henrissat, B. (1996) *Eur. J. Biochem. 263*, 706−713.
8. McCarter, J., and Withers, S. G. (1994) *Curr. Op. Struct. Biol. 4*, 885−892.
9. Vocadlo, D. J., MacKenzie, L. F., He, S., Zeikus, G. J., and Withers, S. G. (1998) *Biochem. J. 335*, 449−455.
10. Bravman, T., Mechaly, A., Shulami, S., Belakhov, V., Baasov, T., Shoham, G., and Shoham, Y. (2001) *FEBS Lett. 495*, 115−119.
11. Botti, M. G., Taylor, M. G., and Botting, N. P. (1995) *J. Biol. Chem. 270*, 20530−20535.
12. Chauvaux, S., Beguin, P., and Aubert, J.-P. (1992) *J. Biol. Chem. 267*, 4472−4478.
13. Belaich, A., Fierobe, H. P., Baty, D., Busetta, B., Bagnara-Tardif, C., Gaudin, C., and Belaich, J.-P. (1992) *J. Bacteriol. 174*, 4677−4682.
14. Davies, G., Sinnott, M. L., and Withers, S. G. (1998) in *Comprehensive Biological Catalysis* (Sinnott, M. L., Ed.) pp 119−208, Academic Press, New York.
15. Vocadlo, D. J., Davies, G. J., Laine, R., and Withers, S. G. (2001) *Nature 412*, 835−838.
16. Kempton, J. B., and Withers, S. G. (1992) *Biochemistry 31*, 9961−9969.
17. Tull, D., and Withers, S. G. (1994) *Biochemistry 33*, 6363−6370.
18. Leatherbarrow, R. J. (1996) *GraFit 3.09b*, Erithacus Software Ltd. Surrey, U.K.
19. Lee, Y.-E., and Zeikus, J. G. (1993) *J. Gen. Microbiol. 139*, 1235−1243.
20. Malet, C., and Planas, A. (1997) *Biochemistry 36*, 13838−13848.
21. Yang, Y., and Hamaguchi, K. (1980) *J. Biochem. (Tokyo) 87*, 1003−1014.
22. Mock, W. L., and Stanford, D. J. (1996) *Biochemistry 35*, 7369−7377.
23. Joshi, M. D., Sidhu, G., Pot, I., Brayer, G. D., Withers, S. G., and McIntosh, L. P. (2000) *J. Mol. Biol 299*, 255−279.
24. Bartik, K., Redfield, C., and Dobson, C. M. (1994) *Biophys. J. 66*, 1180−1184.
25. McIntosh, L. P., Hand, G., Johnson, P. E., Joshi, M. D., Korner, M., Plesniak, L. A., Ziser, L., Wakarchuk, W. W., and Withers, S. G. (1996) *Biochemistry 35*, 9958−9966.
26. Lawson, S. L., Wakarchuk, W. W., and Withers, S. G. (1996) *Biochemistry 35*, 10110−10118.
27. Utt, E. A., Eddy, C. K., Keshav, K. F., and Ingram, L. O. (1991) *Appl. Environ. Microbiol. 57*, 1227−1234.
28. Koshland, D. E. (1953) *Biol. Rev. 28*, 416−436.
29. Sulzenbacher, G., Driguez, H., Henrissat, B., Schulein, M., and Davies, G. J. (1996) *Biochemistry 35*, 15280−15287.
30. Sidhu, G., Withers, S. G., Nguyen, N. T., McIntosh, L. P., Ziser, L., and Brayer, G. D. (1999) *Biochemistry 38*, 5346−5354.
31. Sabini, E., Sulzenbacher, G., Dauter, M., Dauter, Z., Jorgensen, P. L., Schulein, M., Dupont, C., Davies, G. J., Wilson, K. S., and Davies, G. J. (1999) *Chem. Biol. 6*, 483−492.
32. Dale, M. P., Kopfler, W. P., and Byers, L. D. (1986) *Biochemistry 25*, 2522−2529.
33. Dale, M. P., Ensley, H. E., Kern, K., Sastry, K. A. R., and Byers, L. D. (1985) *Biochemistry 24*, 3530−3539.
34. Li, B. F., Holdup, C. A., Morton, C. A., and Sinnott, M. L. (1989) *Biochem. J. 260*, 109−114.
35. Sinnott, M. L., and Souchard, I. J. L. (1973) *Biochem. J. 133*, 89−98.
36. Amyes, T. L., and Jencks, W. P. (1989) *J. Am. Chem. Soc. 111*, 7888−7900.

BI020077V